A global analysis of factors controlling VIIRS nighttime light levels from densely populated areas

Noam Levin [a,b,*], Qingling Zhang [c,d]

[a] Department of Geography, The Hebrew University of Jerusalem, Israel
[b] School of Geography, Planning and Environmental Management, Center of Excellence for Environmental Decisions, The University of Queensland, Australia
[c] Center for Geo-spatial Information, Shenzhen Institutes of Advanced Technology, Chinese Academy of Sciences, Shenzhen, China
[d] Xinjiang Institute of Ecology and Geography, Chinese Academy of Sciences, Urumqi 830011, China

ARTICLE INFO

ABSTRACT

Remote sensing of nighttime lights has been shown as a good surrogate for estimating population and economic activity at national and sub-national scales, using DMSP satellites. However, few studies have examined the factors explaining differences in nighttime brightness of cities at a global scale. In this study, we derived quantitative estimates of nighttime lights with the new VIIRS sensor onboard the Suomi NPP satellite in January 2014 and in July 2014, with two variables: mean brightness and percent lit area. We performed a global analysis of all densely populated areas (n = 4153, mostly corresponding to metropolitan areas), which we defined using high spatial resolution Landscan population data. National GDP per capita was better in explaining nighttime brightness levels ($0.60 < Rs < 0.70$) than GDP density at a spatial resolution of 0.25° ($0.25 < Rs < 0.43$), or than a city-level measure of GDP per capita (in proportion to each city's fraction of the national population; $0.49 < Rs < 0.62$). We found that in addition to GDP per capita, the nighttime brightness of densely populated areas was positively correlated with MODIS derived percent urban area ($0.46 < Rs < 0.60$), the density of the road network ($0.51 < Rs < 0.67$), and with latitude ($0.31 < Rs < 0.42$) at $p < 0.001$. NDVI values (representing vegetation cover) were found to be negatively correlated with cities' brightness in winter time ($-0.48 < Rs < -0.22$), whereas snow cover (enhancing artificial light reflectance) was found to be positively correlated with cities' brightness in winter time ($0.17 < Rs < 0.35$). Overall, the generalized linear model we built was able to explain >45% of the variability in cities' nighttime brightness, when both physical and socio-economic variables were included. Within the generalized linear model, the percent of national GDP derived from income (rents) from natural gas and oil, was also found as one of the statistically significant variables. Our findings show that cities' nighttime brightness can change with the seasons as a function of vegetation and snow cover, two variables affecting surface albedo. Explaining cities' nighttime brightness is therefore affected not only by country level factors (such as GDP), but also by the built environment and by climatic factors.

© 2017 Elsevier Inc. All rights reserved.

1. Introduction

Artificial nighttime lights present one of humanity's unique footprints that can be seen from space (Croft, 1978). Resulting light pollution has been shown to negatively impact the community of astronomers and our ability to observe the night sky (Cinzano et al., 2001). However, the negative effects that light pollution has on ecological systems and on our health, through changes in circadian exposure to light and changes in the wavelengths we are exposed to, might have more important and far-reaching consequences (Longcore and Rich, 2004; Falchi et al., 2011; Gaston et al., 2013). Light pollution and artificial lighting has been shown to vary greatly in space and in time, as a function of population and economic activity. However, most studies examining the factors explaining global spatial variability in lit areas were conducted at national and provincial levels using the DMSP/OLS sensor (e.g., Elvidge et al., 1997; Chen and Nordhaus, 2011; Wu et al., 2013; Keola et al., 2015). While offering the only globally available time series of nighttime lights imagery from 1992 onwards (Bennie et al., 2014a), DMSP imagery has various drawbacks as it is not calibrated, its spatial resolution is coarse, it contains overglow beyond urban boundaries and it is saturated in urban areas (Small et al., 2005; Doll, 2008). Temporal changes in cities' lights and the spatial characteristics of cities' nighttime brightness have been examined in several countries using DMSP data

* Corresponding author.
E-mail address: noamlevin@mscc.huji.ac.il (N. Levin).

(e.g., Lo, 2002; Ma et al., 201?; Zhang and Seto, 2013). Most of the studies which used DMSP data for urban studies have used annual datasets, whereas daily and monthly datasets were used to identify more dynamic and time varying features, such as forest fires, wars and fishing vessels (Huang et al., 2014). New studies using DMSP datasets for quantifying urban patterns are continuously being published (e.g., Ma et al., 2015; Weidmann and Schutte, 2016), however, annual products of DMSP night lights data are no longer being produced, the last one available being that of 2013.

Recently, new studies have attempted using finer spatial resolution (≤1 m) nighttime imagery to examine the factors explaining spatial patterns of nighttime lights within cities (Kuechly et al., 2012; Hale et al., 2013; Levin et al., 2014; Katz and Levin, 2016). Astronaut photography taken from the International Space Station presents an additional source of information about spatial patterns of cities at nighttime (de Miguel et al., 2014, de Miguel, 2015). Levin and Duke (2012) have used ISS imagery showing that not all towns and cities are equally lit, and that economic, infrastructure and demographic factors can explain differences in brightness levels of localities in Israel and the West Bank. Kyba et al. (2014) have used VIIRS DNB data to study the relationship between population size and the sum of lights from cities and communities in the USA and
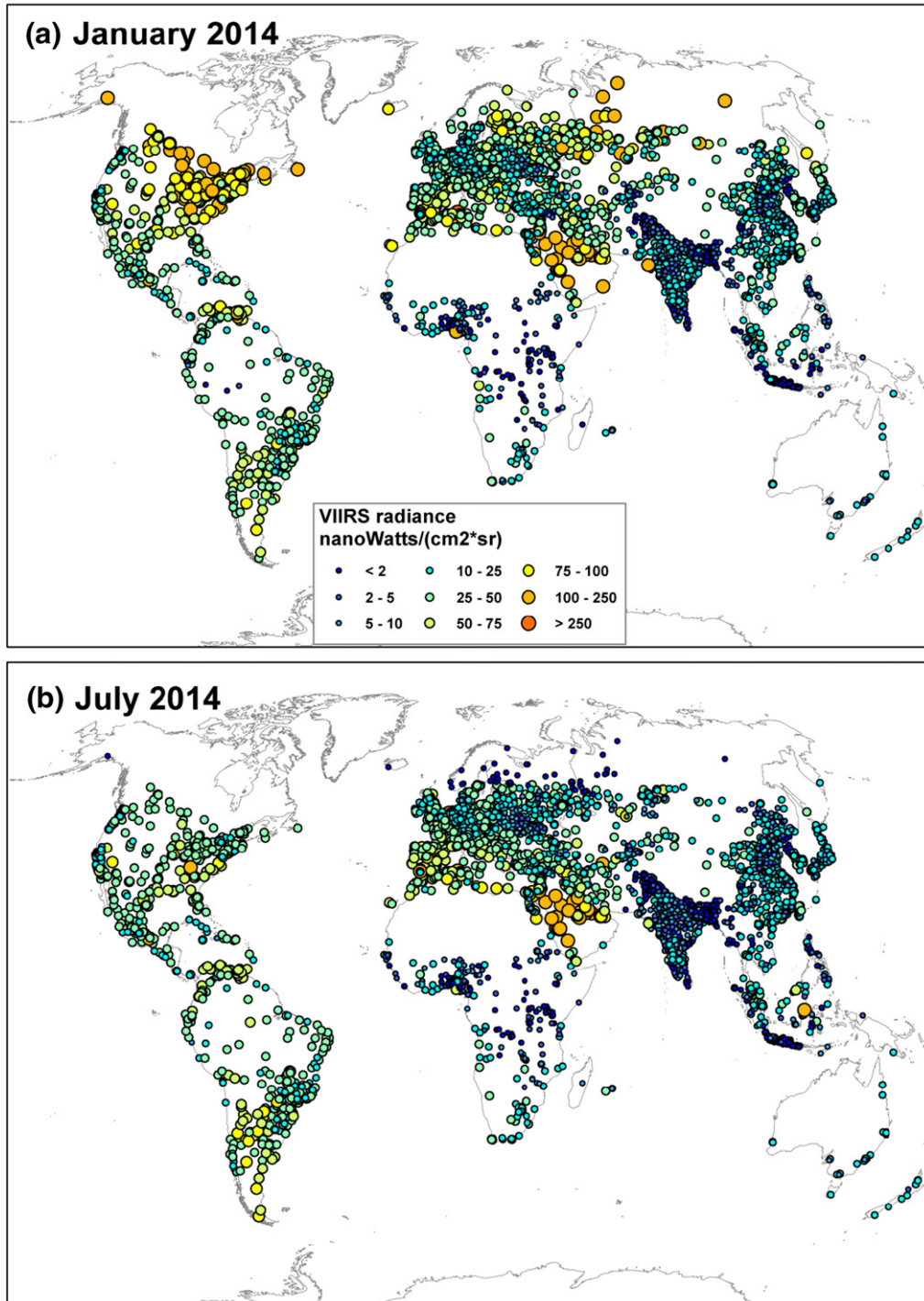
Fig. 1. The distribution of the 4153 urban areas analyzed in this study, presenting mean VIIRS radiance values in January 2014 (a) and in July 2014 (b). Changes in brightness between the two months are given in absolute values (c) and as percentages (d).
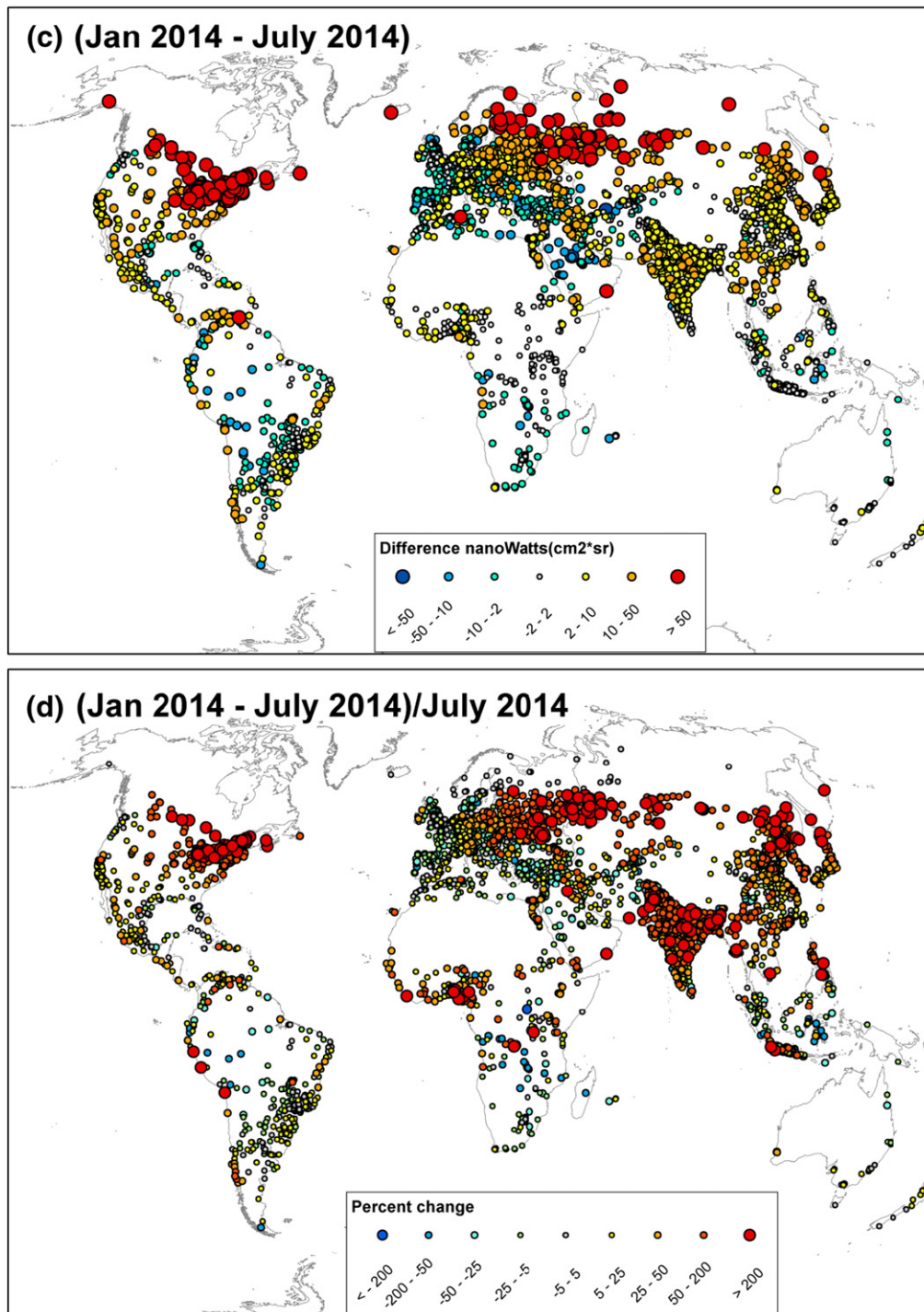
Fig. 1 (*continued*).

Germany, finding differences in light emission between cities of these two countries, and several recent studies have used VIIRS data to examine the nighttime brightness of cities in China (Ma et al., 2014a, 2014b; Shi et al., 2014a, 2014b) and in the USA (Chen et al., 2015). In addition, Elvidge et al. (2016) have used VIIRS data to detect and measure radiant emissions from gas flares globally, forming one of the major industrial sources of light pollution,

which can even be detected night-time images of Landsat 8 in the visible bands (Levin and Phinn, 2016).

Urban areas are of high importance as most of the world's population resides in cities, with 78% of global carbon emissions attributed to cities (Grimm et al., 2008). In this paper our aim was to use the new monthly global cloud-free mosaics from the VIIRS sensor onboard the Suomi-NPP (launched in 2011), to examine the factors

Fig. 2. VIIRS radiance values in January 2014 (first and third row) and Landscan population density (per square kilometer; second and fourth row) in 2012 in six selected urban areas, ordered by their brightness from the top-left (Chicago) to the bottom-right (Moscow). The grey lines delineate the urban areas as defined based on the global Landscan population data (see Methods).
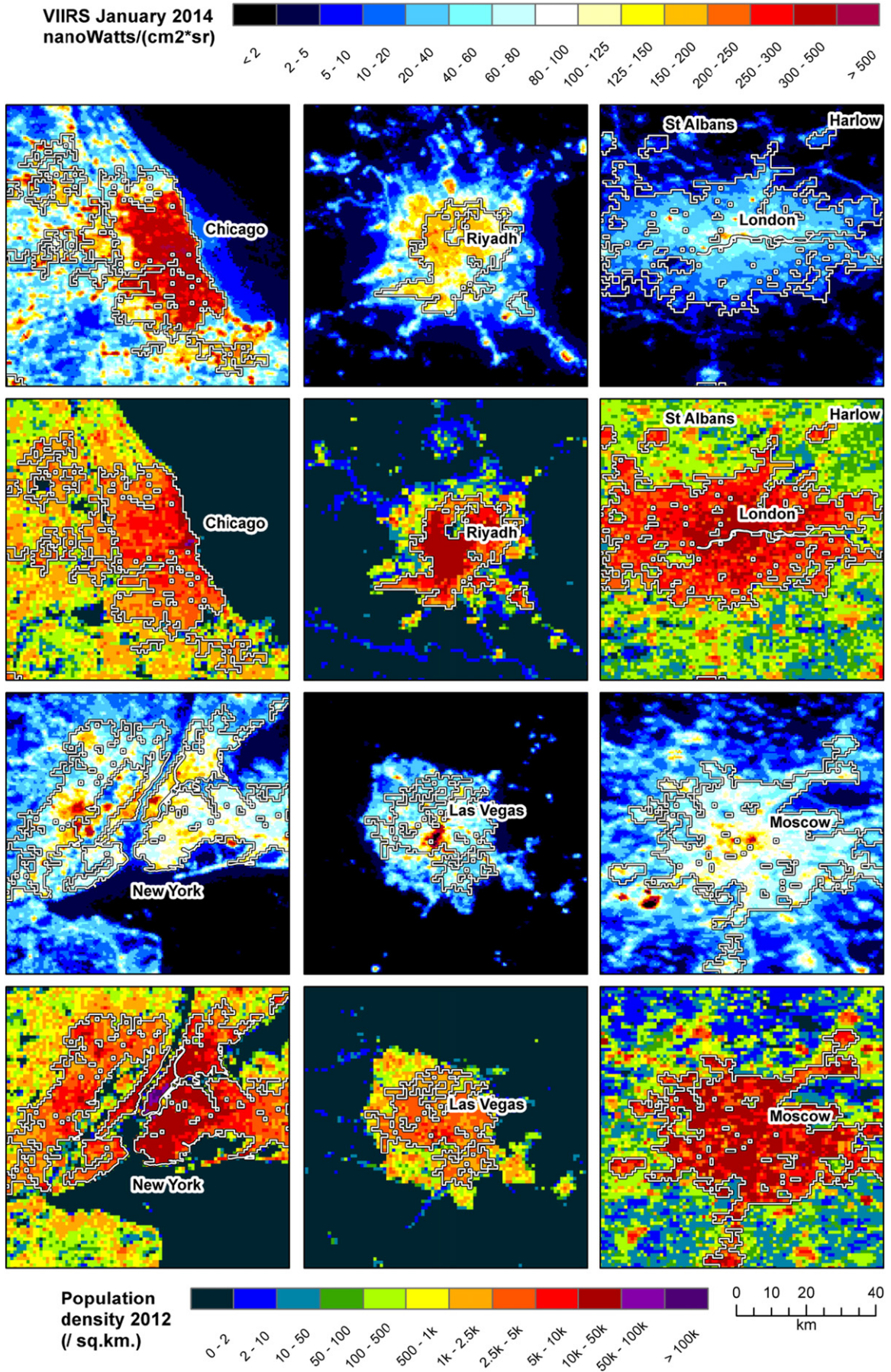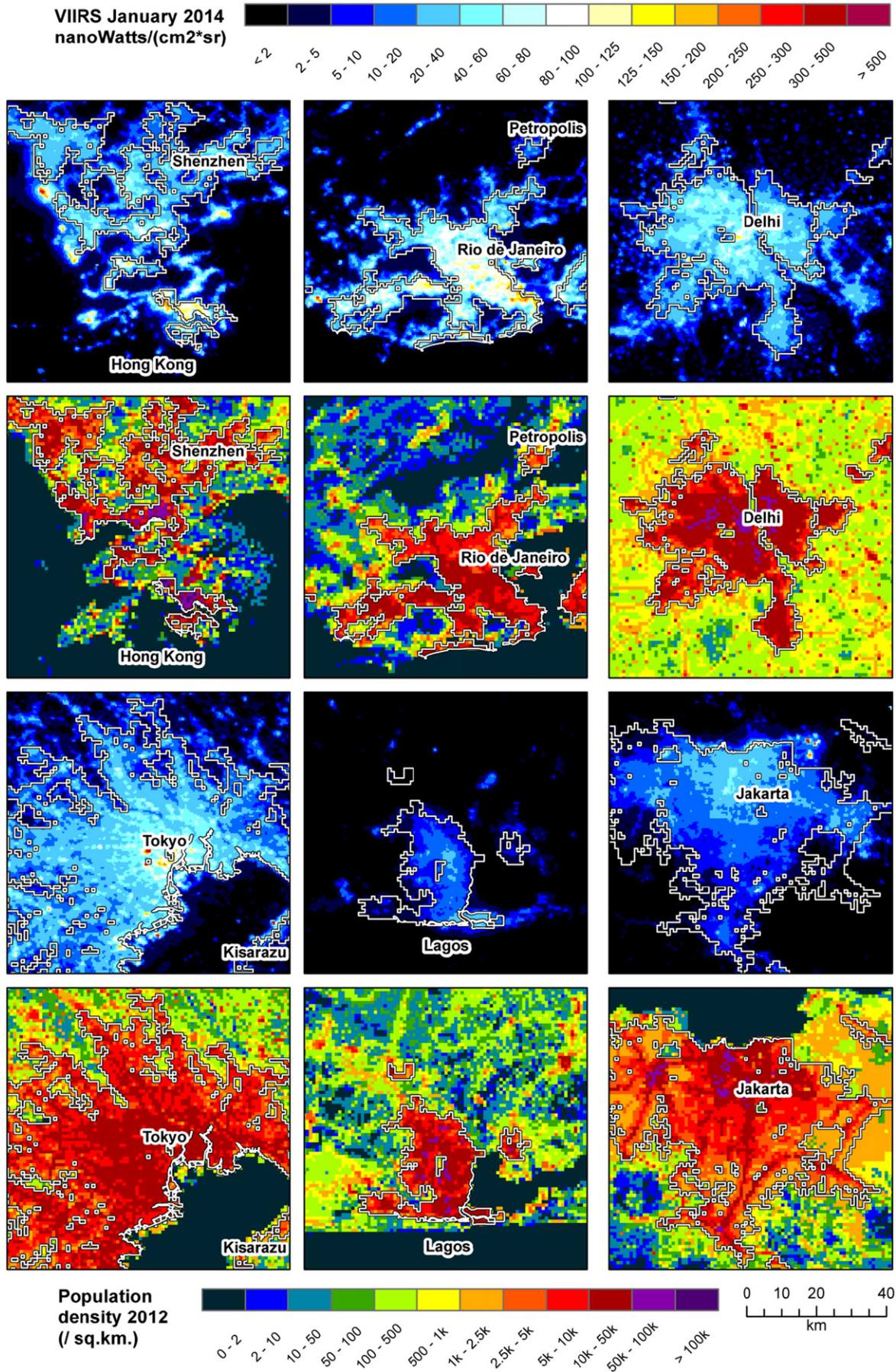
explaining spatial variability in nighttime lights at the city level, comparing densely populated areas (mostly urban areas) globally. We hypothesized that urban form and urban density (and other factors including percent urban area, NDVI, snow cover etc.) will also affect brightness levels, and not just socio-economic factors such as national GDP and population size. In addition, we aimed to examine the difference between using lit areas (i.e., areas above a certain threshold of nighttime lights brightness, as usually done in studies using DMSP data) and using calibrated brightness levels in radiance values, on the resulting factors explaining inter-city variability in nighttime lights.

2. Methods

The Visible/Infrared Imager/Radiometer Suite (VIIRS) was launched in October 28, 2011, collecting high quality nighttime images at a spatial resolution of 750 m in the Day/Night Bands (DNB), between 500 and 900 nm (Miller et al., 2012, 2013). Recent studies have shown the improved quality of VIIRS nighttime lights images over those acquired by the DMSP/OLS sensor (Elvidge et al., 2013; Li et al., 2013; Miller et al., 2013; Shi et al., 2014a, 2014b). There are now monthly cloud-free global calibrated mosaics that were compiled from nighttime lights VIIRS images (Baugh et al., 2013), which can be downloaded from the NOAA's National Geoscience Data Center (http://ngdc.noaa.gov/eog/). We have downloaded Version 1 of the composites of January 2014 (representing northern hemisphere winter when snow cover is high) and July 2014 (representing northern hemisphere summer), to quantify the nighttime light brightness of urban and densely populated areas globally.

To define the densely populated areas to be analyzed, we used the global Landscan (Bhaduri et al., 2002) population layer (of 2012; http://web.ornl.gov/sci/landscan/). Landscan is a derived product based on a variety of different inputs (including roads, land cover and other remote sensing products) used to spatially disaggregate census data (Bhaduri et al., 2002). Instead of defining the cities to be analyzed using official municipal boundaries (which often include unbuilt areas, and split metropolitan areas into small units; Forstall et al., 2009) we defined densely populated areas (to which we refer as "cities" throughout the paper) as comprised of adjacent grid cells with >1500 people/km^2 each (the threshold used in China to define urban areas; Chan and Hu, 2003), with a minimum total area of 10 km^2 within a single country. For comparison, Angel et al. (2011) mapped 3646 metropolitan areas globally with populations in excess of 100,000 people, finding that their median density was 7600 people/km^2. The steps for generating this spatial layer of cities were the following: (1) we calculated population density within each grid cell of the Landscan population dataset, by dividing the population count of each cell by the area of each 30 arc-seconds cell; (2) we used the post-classification sieve function within Envi 5.2 (2014 Exelis) to keep only groups of 25 (or more) adjacent grid cells each with >1500 people/km^2 (considering 4 neighboring cells); (3) the resulting binary image was converted to a polygon layer which was intersected with countries' boundaries; (4) finally, only those polygons (representing densely populated areas) whose area within a single country was >10 km^2, were then used for all analyses (n = 4153). Using this approach, our analysis units often correspond to metropolitan areas.

For each of the resulting polygons, we calculated various statistics (minimum, maximum, mean, standard deviation, sum) using the Zonal Statistics tool within ArcGIS 10.2 (ESRI, Redlands, CA) for three groups of variables:

1) Anthropogenic variables at the city level: area, population, population density, percent urban area, density of road network, and GDP density at grid cell resolution of 0.25 degrees (projected to 2014, based on Gaffin et al., 2004). We used percent urban areas based on the 2013 MODIS Land Cover Type Product (MCD12Q1; Strahler et al., 1999) because it was found as a highly accurate global map of urban areas in an accuracy assessment performed by Potere et al. (2009). For assessing the density of road network within each city, we used shapefiles of OpenStreetMap (Haklay, 2010) obtained from Geofabrik (http://www.geofabrik.de/). The roads within OpenStreetMap are classified as Major roads (Motorway/freeway; Important roads, typically divided; Primary roads, typically national; Secondary roads, typically regional; Tertiary roads, typically local) and Minor roads (Smaller local roads; Roads in residential areas; Streets where pedestrians have priority over cars; Pedestrian only streets) (Ramm, 2015). We converted the layers of major roads and minor roads from polylines to points (using all vertices), and then counted the number of vertices in each of these layers within each 0.00083 × 0.00083 degree grid cell (as in Levin et al., 2015). In addition we classified the VIIRS nighttime light images into radiance classes, calculating the percent lit area of each city above the following light levels: 2, 5, 10, 25, 50, 100 and 250 nW/(cm^2 * sr). We identified active gas flare sources within cities using the global mapping of gas flares provided by Elvidge et al. (2016), available for download here: http://www.mdpi.com/1996-1073/9/1/14/s1 (accessed on December 7th, 2016). Out of a total of 7464 gas flare point sources, only 97 gas flare sources were found within the boundaries of 75 densely populated areas included in our study. To examine the possible impact of gas flares on our results, we examined the statistical correlations with and without cities where gas flare sources were located.

2) Physical variables at the city level: VIIRS nighttime lights brightness, the 2014 NDVI values (Rouse et al., 1973) based on the Version 6 of the MODIS/Terra Vegetation Indices Monthly L3 0.05Deg CMG (MOD13C2) collection (Didan, 2015) as vegetation cover can absorb and block nighttime lights, and snow cover based on the 2014 MOD10CM product of MODIS as snow cover can enhance surface reflectance. Whereas spring-time snow cover in the northern hemisphere has decreased between 1971 and 2014, winter-time snow cover in the northern hemisphere showed only weak trends (Hernández-Henríquez et al., 2015). For each of the cities, we calculated its mean snow cover and mean NDVI values in January and July 2014. We also calculated for each city the number of cloud-free coverages, or observations, that went in to constructing the average VIIRS radiance image, because cloud cover can impede observations of nighttime brightness.

3) Anthropogenic variables at the country level, based on the assumption that street lighting standards and types are related to a country's national income and energy sources. Street design standards are deeply embedded in design and engineering practices, as well as in legal and financial structures (Southworth and Ben-Joseph, 1995), and thus we assumed that street lighting standards will be mostly directed by national guidelines and norms. The variables we examined at the national level were GDP per capita and the percent of GDP derived from income (rents) from natural gas and oil. The variables of 'GDP per capita' and 'Percent of GDP derived from natural gas and oil rents' were only available at the country scale, and were thus assigned to each city based on its country. The motivation for examining the percent of GDP derived from income (rents) from natural gas and oil, was that major oil exporting countries are known as non-efficient in their

Fig. 3. VIIRS radiance values in January 2014 (first and third row) and Landscan population (per square kilometer, second and fourth row) in 2012 in six selected urban areas, ordered by their brightness from the top-left (Hong Kong) to the bottom-right (Jakarta). The grey lines delineate the urban areas as defined based on the global Landscan population data (see Methods). VIIRS radiance values for Jakarta are from July 2014, due to low cloud-free coverage in January 2014.
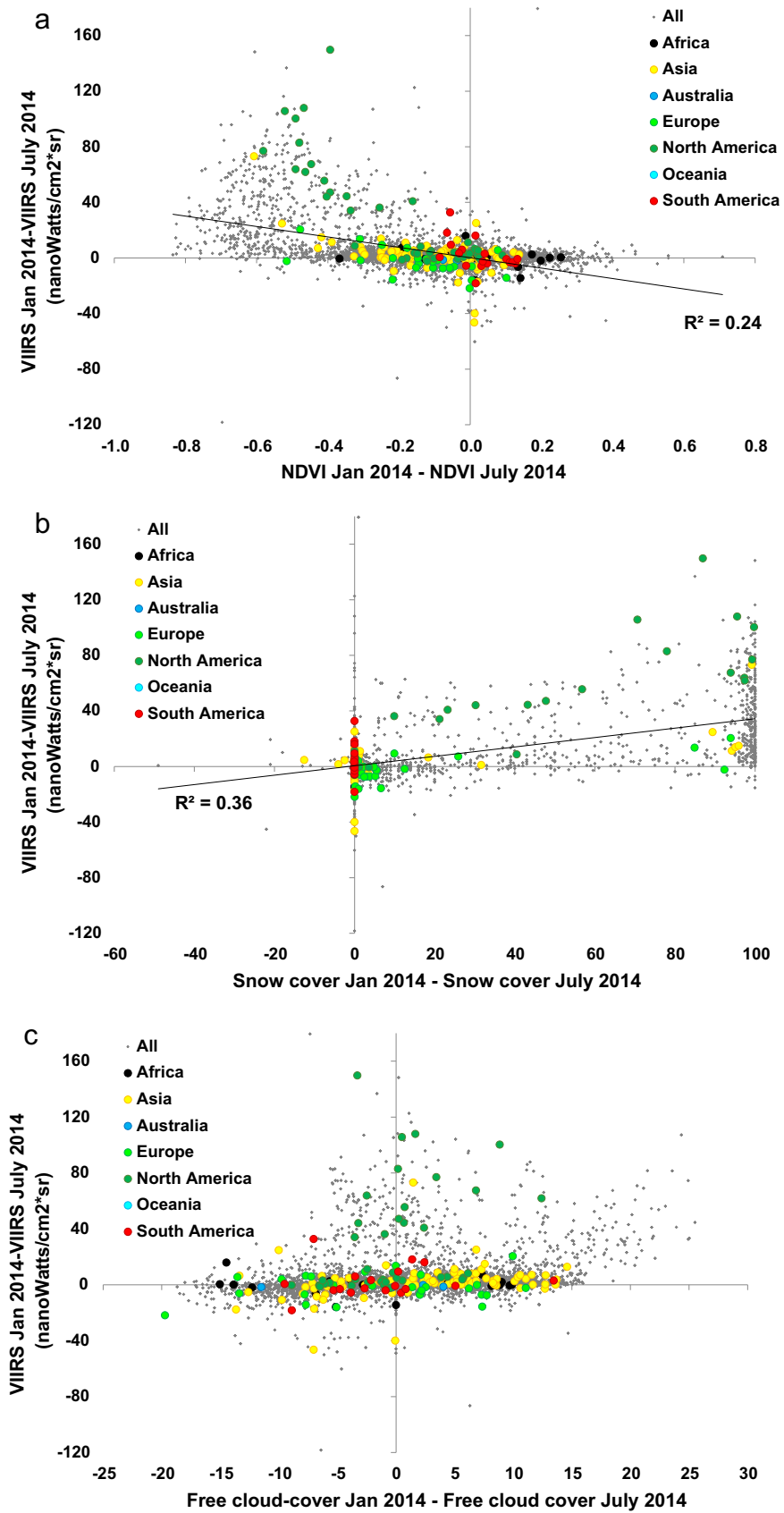
Fig. 4. Changes in VIIRS brightness values between January 2014 and July 2014, as a function of: (a) changes in NDVI values; (b) changes in snow cover values; (c) changes in cloud-free coverage. The largest 200 cities are colored by their respective continent.

Table 1

Spearman rank correlation coefficients between explanatory variables and mean VIIRS radiance values (in January and July 2014), at different spatial scales (individual cities, average for cities within countries). The variables of 'GDP per capita' and 'Percent of GDP derived from natural gas and oil rents' were only available at the country scale, and were thus assigned to each city based on its country.

	City level, n = 4153		City level, n = 200 largest		Country level, n = 170	
	Mean VIIRS Jan 2014	Mean VIIRS July 2014	Mean VIIRS Jan 2014	Mean VIIRS July 2014	Mean VIIRS Jan 2014	Mean VIIRS July 2014
GDP per capita	0.637[***]	0.657[***]	0.604[***]	0.627[***]	0.694[***]	0.697[***]
GDP density	0.264[***]	0.291[***]	0.433[***]	0.433[***]	0.395[***]	0.362[***]
GDP per capita % of city's share of national population[*]	0.532[***]	0.619[***]	0.494[***]	0.577[***]	0.581[***]	0.618[***]
Percent of GDP derived from natural gas and oil rents	0.039[*]	−0.069[***]	−0.062	−0.129	0.309[***]	0.278[***]
Area km^2	0.083[***]	0.118[***]	−0.029	−0.046	0.071	0.099
Population density	0.046[**]	0.057[***]	−0.073	−0.100	−0.178[*]	−0.175[*]
% urban area	0.576[***]	0.596[***]	0.582[***]	0.555[***]	0.461[***]	0.498[***]
Major roads	0.583[***]	0.667[***]	0.586[***]	0.619[***]	0.513[***]	0.581[***]
Mean NDVI	−0.405[***]	−0.237[***]	−0.485[***]	−0.260[***]	−0.220[**]	−0.142
Mean snow	0.334[***]	0.032[*]	0.348[***]	−0.034	0.175[*]	0.028
Latitude (abs)	0.386[***]	0.309[***]	0.351[***]	0.313[***]	0.416[***]	0.386[***]
Number of VIIRS cloud-free coverages	0.230[***]	0.461[***]	0.194[**]	0.507[***]	0.367[***]	0.444[***]

[***] $p < 0.001$.
[**] $p < 0.01$.
[*] $p < 0.05$.

energy use (Doukas et al., 2006; Mehrara, 2007), and we hypothesized that artificial night-lights emissions will also reflect the high energy consumption of some of those countries. Recognizing however that GDP varies within a country, in addition to using gridded GDP density at a spatial resolution of 0.25° (by Gaffin et al., 2004, as described above), we used for some of the analyses GDP per capita as of 2014 at the city level, available for the world's 300 largest metropolitan economies (Parilla et al., 2015; https://www.brookings.edu/research/global-metro-monitor/, accessed August 18th, 2016). As city-level GDP from the Brookings Institute was available for only 300 cities, we could not use it in the analysis of all cities. We have also assigned each city with its country-level GDP per capita value in proportion to each city's fraction of the national population, as an additional measure of GDP per capita at the city level.

We examined the correlations between the explanatory variables of population, percent urban area, road density, NDVI, snow over, GDP per capita, GDP density as of 2014 (GDP/unit land area; calculated by interpolating the 1990 and 2025 GDP density values at 0.25° grid cell resolution from Gaffin et al., 2004), percent of GDP derived from income (rents) from natural gas and oil (average between 2010 and 2013,

available from the World Bank, http://data.worldbank.org/indicator/, accessed on 21/7/2015) and number of cloud free coverages from which the monthly mosaics of VIIRS brightness were constructed, with the predicted variables of nighttime light brightness, and lit area, at two spatial scales: the city scale (n = 4153, and n = 200 for the largest urban areas globally) and the country scale after averaging the various variables of all cities within each country (n = 170). At the country level we examined the statistical relationships averaging the major cities in each country, and not referring to the entire area of a country. While previous studies trying to explain nighttime lights often focused on total lit area (as in Elvidge et al., 1997) or on the sum of lights (as in Kyba et al., 2014), we aimed to explain the percent lit area within a city and the mean radiance light levels within cities – variables which will be less biased by a city's total population. We used XLSTAT version 2014.6.01 (Copyright Addinsoft 1995–2014) to calculate Spearman's rank correlation coefficients.

Following the univariate statistical analysis, we ran general linear models (GLM) for explaining cities' brightness. Because seasons in the northern and in the southern hemispheres are reversed, we first reorganized data by seasons (winter and summer) instead of months
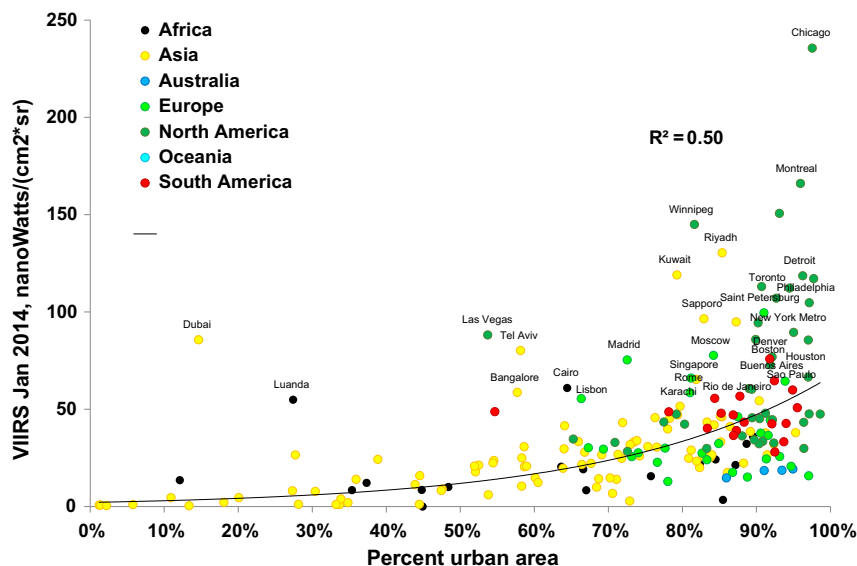

Fig. 5. Mean VIIRS radiance values in January 2014 in the 200 largest urban areas, as a function of percent urban area.

(January and July). To do that we switched all data acquired in winter with data acquired in summer in the southern hemisphere. We then standardized all data using the Gaussian standardization method. We built GLM models (using the GLM function in Matlab) including all variables (full models), including social-economic variables only (socio-economic models), and including physical variables only (physical models). After examining distributions of the VIIRS data, we decided to choose a normal type for all the GLM models. To examine the performances of all the models, we listed all parameters of the models and generated scatterplots with the observed VIIRS data (Y axis) and the predicted values (X axis). GLM models were run for all cities, for the largest 200 cities, as well as at the country level.

3. Results

3.1. City level

Altogether, we identified 4153 populated areas globally, mostly corresponding to cities and metropolitan areas (Fig. 1; see Supplementary KML file for the polygons of all cities). Their median area

was 29.3 km^2 (with a maximum of 3927 km^2, for Jakarta, Indonesia), their median population being 172,000 (with a maximum of 30.4 million people for Tokyo, Japan), the median population density being 5476 people/km^2 (with a maximum of 39,605 people/km^2 for Hong Kong), and the median brightness of these cities was 19 and 16.5 nW/(cm^2 ∗ sr) in January and July 2014, respectively (Figs. 2, 3, S1). The overall population included within these 4153 populated areas was 2.018 billion, 30% of the world's population. Whereas in some of the metropolitan areas (as defined in this study) such as Jakarta, there were areas which were quite dark, in some of the metropolitan areas (e.g., Ryadh and Moscow), very bright areas extended beyond the populated areas (Figs. 2, 3).

Using at least two cloud free coverages within a monthly mosaic as a threshold (representing a higher signal to noise ratio), 3955 (95%) and 3871 (93%) of all cities (in January and July 2014, respectively), and 188 (94%) and 192 (96%) of the largest 200 cities (in January and July 2014, respectively), were above this threshold. We examined all univariate correlations only for those cities above this threshold, and found (as shown in the Supplementary tables) that the univariate correlations between the explanatory variables and with VIIRS night-time brightness levels were
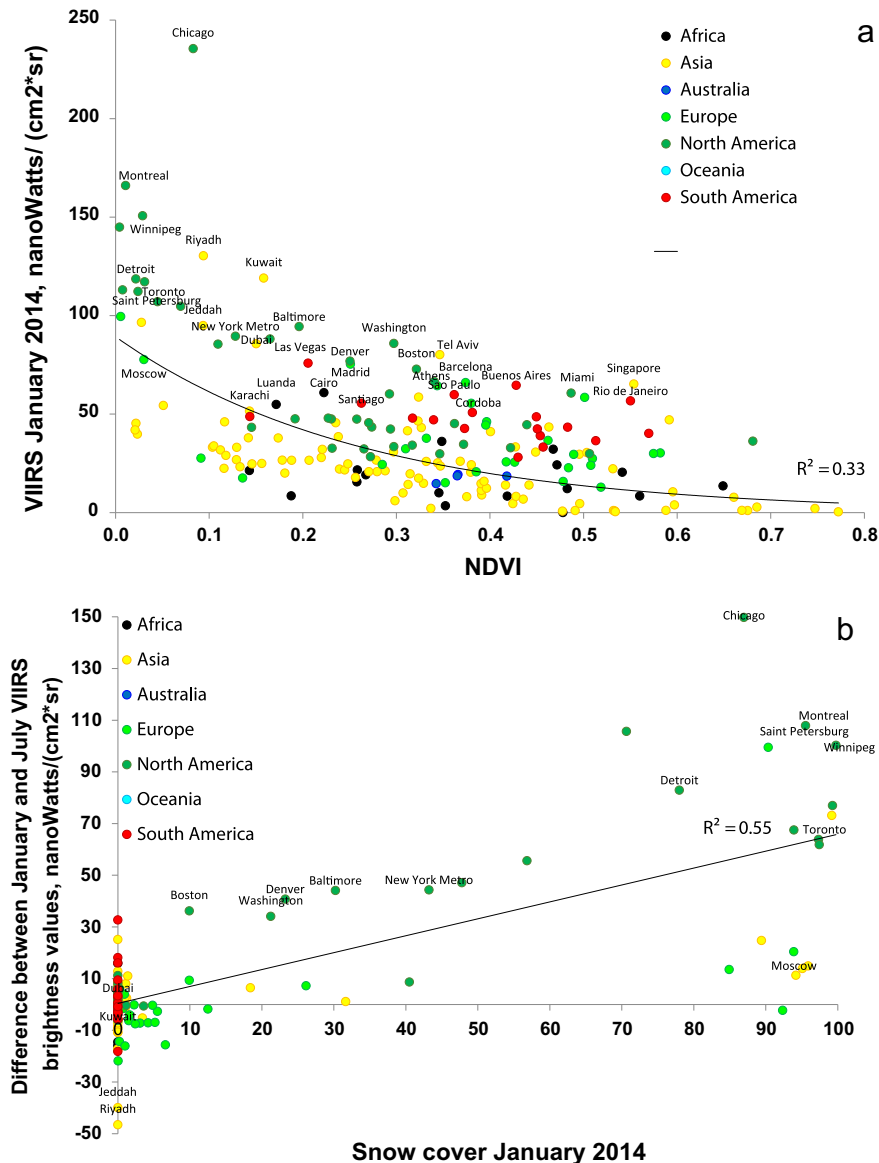

Fig. 6. Mean VIIRS radiance values in January 2014 in the 200 largest urban areas, as a function of mean NDVI values (a); Difference between January and July VIIRS brightness values in the largest 200 urban areas, as a function of snow cover in January 2014 (b).

not affected by low cloud free coverage. Using only cities with no gas flare sources, 4078 (98%) of all cities, and 181 (91%) of the largest 200 cities, were found to have no artificial lights from gas flares. We examined all univariate correlations only for those cities with no gas flare sources, and found (as shown in the Supplementary tables) that the univariate correlations between the explanatory variables and with VIIRS night-time brightness levels were not affected by gas flare sources.

Globally, a consistent spatial pattern was observed with high-latitude northern hemisphere cities being observed as brighter on the January 2014 image than on the July 2014 image (Fig. 1c, d). Changes in VIIRS brightness values between January and July 2014, were significantly correlated with changes in NDVI values ($Rs = -0.405$, $p < 0.001$), changes in snow cover ($Rs = 0.358$, $p < 0.001$) and with changes in cloud-free coverage ($Rs = 0.315$, $p < 0.001$) (Fig. 4).

We found statistically significant correlations for most of the variables analyzed for the VIIRS nighttime lights variables of both January and July 2014. However the variables of area, population density and percent of GDP derived from natural gas and oil rents were the least strongly correlated variables when each variable was examined separately (Table 1). Nighttime light brightness of cities was positively correlated with national GDP per capita ($0.60 < Rs < 0.66$; but less so with GDP density: $0.26 < Rs < 0.43$), percent urban area ($0.55 < Rs < 0.60$; Figs. 5, S2), road density ($0.58 < Rs < 0.67$) and snow cover (Fig. 6; $R^2 = 0.55$), and negatively (albeit weakly) correlated with NDVI values (Figs. 6, S4; Table 1). Examining the correspondence of GDP per capita data and VIIRS night-time brightness for the 285 cities for which there was GDP per capita data at the city level (from the Brookings Institution; Parilla et al., 2015), GDP per capita at the city level was correlated with VIIRS night-time brightness ($Rs = 0.339$ and 0.220, $p < 0.001$, for January and July, respectively), but it was not significantly a better predictor of VIIRS night-time brightness, than GDP per capita at the national level ($Rs = 0.307$ and 0.203, $p < 0.001$, for January and July, respectively Table S3) for those 285 cities. In addition, the correlation coefficient between the city-level measure of GDP per capita (in proportion to each city's fraction of the national population) with night-time brightness, was lower than the correlation coefficient between the simple national GDP per capita with night-time brightness (see tables S1, S2). National GDP per capita was highly correlated with GDP density ($Rs = 0.645$, $p < 0.001$) and with the city-level measure of GDP per capita (in proportion to each city's fraction of the national population; $Rs = 0.644$, $p < 0.001$). We therefore preferred to keep using national GDP per capita assigned to each city in our following multivariate analyses, to avoid collinearity.

VIIRS brightness values were highly correlated between January 2014 and July 2014, the main outliers presenting higher brightness values in January being cities located in northern latitudes with high snow cover (Figs. 1c,d, 7). Correlations between the explanatory variables and the nighttime light variables (of mean radiance values and of lit area) did not differ much, however the highest correspondence between mean VIIRS radiance values and percent lit area was obtained for lit areas above 10–100 $nW/(cm^2 * sr)$ (Fig. 8; Table S1, S2, S4), and the relationship between lit area and mean brightness levels was found to be non-linear (Fig. 9). In the GLM analysis (run separately for all cities, or just for the largest 200 cities), both physical and socio-economic variables were found as statistically significant (Fig. 10). At the city level, the adjusted Rsquared value of a GLM model was mostly higher when only physical variables were included, than when only socio-economic variables were included (Fig. 11). However, in all cases, the explanatory power of the model increased when both socio-economic variables and physical variables were combined in a full GLM model (adjusted R^2 values increasing from between 0.29–0.43 to 0.46–0.63 in the full GLM; Figs. 10, 11, S4). Amongst the physical variables, NDVI and major roads were statistically significant in all models in both seasons, whereas cloud-free coverage was more important for the model in the summer season (Fig. 10), and snow cover was only statistically significant in the winter season (Fig. 10; note that the GLM coefficients of snow cover were higher than the GLM coefficients of latitude in the winter season). Amongst the socio-economic variables, both national GDP per capita and the percent of GDP derived from natural gas and oil rents were positively contributing to the explanation of cities' night-time brightness (Fig. 10).

3.2. Country level

In this section we report the results obtained at the country level, i.e. after averaging all cities within each country. Overall, the three leading countries in number of densely populated areas included in our analysis were China (514), India (437) and the USA (306). At the country level (in which we analyzed the major cities in each country, and not the entire area of a country), the brightest cities in July 2014 were all found in the Middle East, whereas in January 2014 some countries located in higher latitudes were also amongst the ones with the brightest cities (Fig. 12; brightness data was not available in July for cities in Iceland, Finland
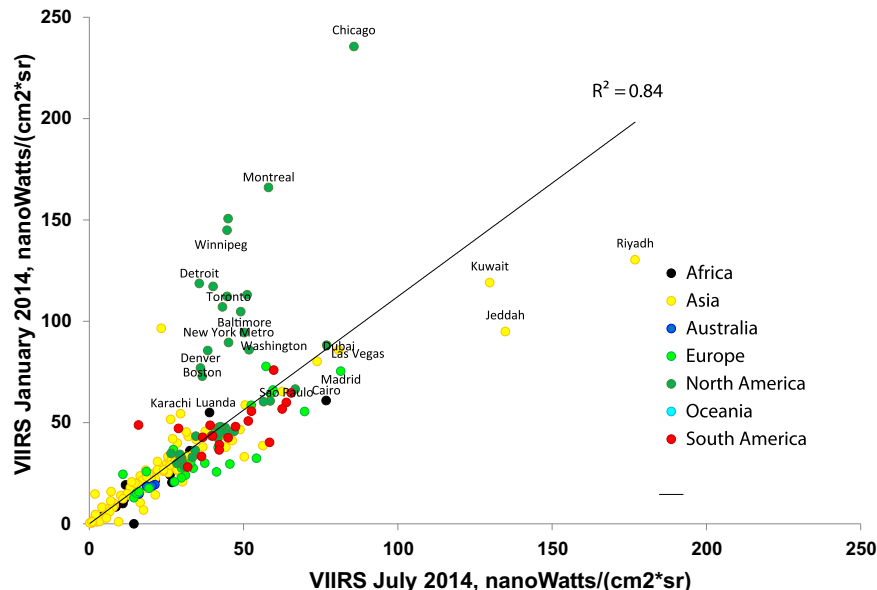

Fig. 7. Mean VIIRS radiance values in January 2014 in the 200 largest urban areas, as a function of mean VIIRS radiance values in July 2014.

and Norway due to long days). At the country level, statistically significant correlations were found for VIIRS nighttime lights for all variables analyzed in both seasons (January and July 2014), except for four variables in which the correlations were weak or non-significant: area, population density, NDVI and snow (Table 1). Nighttime light brightness of cities was positively correlated with GDP per capita (Fig. 13), percent of GDP derived from natural gas and oil rents (Fig. 14), percent urban area (Fig. 15) and road density (Fig. 16, Table 1). At the country level, snow cover and NDVI were only weakly correlated with VIIRS night-time brightness in January, and were not correlated with VIIRS night-time brightness in July (Table 1). VIIRS brightness values were highly correlated between January 2014 and July 2014, the main outliers presenting higher brightness values in January being countries located in northern latitudes with high snow cover in winter-time such as Canada, Estonia and the Russian Federation (Fig. 12). In the GLM analysis, both physical and socio-economic variables were found as statistically significant (Fig. 10). At the country level, the adjusted R^2 value of a GLM model was higher when only socio-economic variables were included, than when only physical variables were included (Fig. 11). However, in all cases, the explanatory power of the model increased when both socio-economic variables and

physical variables were combined in a full GLM (adjusted R^2 values increasing from between 0.24–0.37 to 0.49–0.54 in the full GLM; Figs. 10, 11, S4). Amongst the physical variables, NDVI, cloud-free coverage and major roads were statistically significant in all models in both seasons, whereas snow cover was not found as statistically significant at the country level (Fig. 10). Amongst the socio-economic variables, both national GDP per capita and the percent of GDP derived from natural gas and oil rents were positively contributing to the explanation of cities' nighttime brightness at the country level (Fig. 10).

4. Discussion

Overall, our global mapping identified 4154 densely populated areas, 13.9% more than the 3646 metropolitan urban areas identified by Angel et al. (2011) who used MODIS derived urban land cover and population data. Previous global studies which analyzed differences in nighttime light brightness at the country or state level often focused on four main variables: population size, urban area, GDP and electric power consumption (e.g., Elvidge et al., 1997, 1999; Small et al., 2005; Ma et al., 2012, 2014a). Here we found that population density was not a
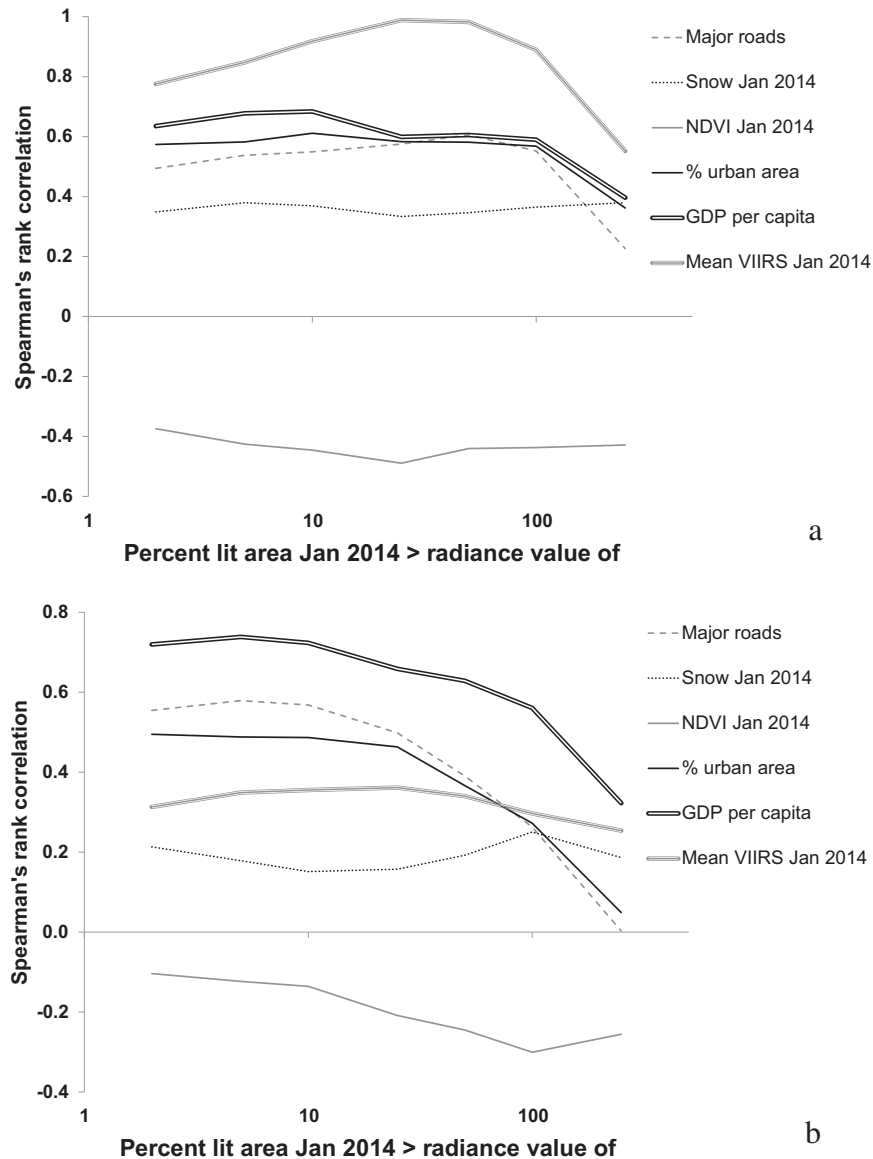

Fig. 8. Spearman rank correlation coefficients between various variables and the percent lit area (in January 2014) as a function of the threshold used to define the percent lit area, in radiance units of nano-Watts/(cm² ∗ sr), for the 200 largest urban areas (a) and for countries (b). The threshold used for defining binary images of lit and unlit areas, from which we calculated the percent lit area, is shown on the x-axis.
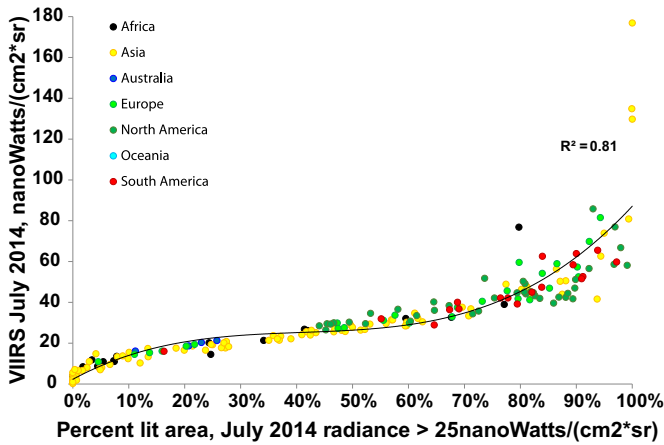
Fig. 9. Mean VIIRS radiance values in July 2014 in the 200 largest urban areas, as a function of the percent lit area >25 nW/(cm^2 ∗ sr).

statistically significant variable for explaining cities' night-time brightness when comparing cities between countries globally; this lack of correlation may be explained by our focus on highly densely populated areas (excluding sparsely populated areas from the analysis), by additional socio-economic factors which are unrelated to population density (e.g., GDP per capita), by physical factors influencing surface albedo (such as snow cover and NDVI), and by the great variability in lighting standards between countries (e.g., lighting levels, distance between street lights, whether there are regulations to reduce light pollution by using full cut-off lamps, etc.), the type of street lighting used (lamp type, which can be identified using hyperspectral imagery; Elvidge et al., 2010), etc. It is worthy of noting that slums with very high population density in many developing country cities are often poorly lit (Jones, 2000). While there are various attempts to map GDP spatially at regional and city levels (Gaffin et al., 2004; Parilla et al., 2015), we found that city level GDP estimates were not better in explaining nighttime brightness of cities, than national GDP per capita values. This

finding may indicate the importance of national lighting standards in explaining cities' nighttime brightness and the percolation of governmental revenue to municipal budgets which are also responsible for street lighting.

We found that there are additional socio-economic factors beyond population size and GDP which explain cities' brightness levels. We have found that cities located in countries where a large percent of the GDP is derived from natural gas and oil rents, tend to be highly lit – this is especially evident in the countries surrounding the Persian Gulf, where oil revenues have led to rapid urban development (Zhang et al., 2015), and where energy consumption and carbon dioxide emissions per capita are high (Reiche, 2010). Indeed, in major oil exporting countries, government policies often drive domestic energy prices under free market level, leading to high levels of domestic energy consumption, and to higher growth rates in energy use per capita than the growth rate of GDP per capita (Mehrara, 2007). Recent studies using finer spatial resolution sources of nighttime lights have incorporated additional explanatory variables which were found to be statistically significant in explaining differences between localities in nighttime light brightness (e.g., house vacancy rates; Chen et al., 2015), with one of the most consistent variables being the density of the road network (Levin and Duke, 2012; Kuechly et al., 2012; Hale et al., 2013; Levin et al., 2014), a variable which was also shown to be statistically significant in our results. Whereas in previous studies official road data sets were used to estimate road density and correlate it with light emission, we used OpenStreetMap data, which has also been recently used to map roadless areas globally (Ibisch et al., 2016). Although the spatial coverage of OpenStreetMap data varies between countries and cities, with most contributors originating from the developed countries (Neis and Zielstra, 2014), our findings indicate that road density as derived OpenStreetMap succeeded in contributing to the explanation of spatial variability in light emission from densely populated areas.

Few studies have explicitly incorporated variables related to surface reflectance to explain nighttime brightness (but see Kim, 2012; Katz and Levin, 2016), and none as far as we know have done this at the global scale. We found that NDVI (representing vegetation cover) was negatively correlated with nighttime brightness, whereas snow cover was
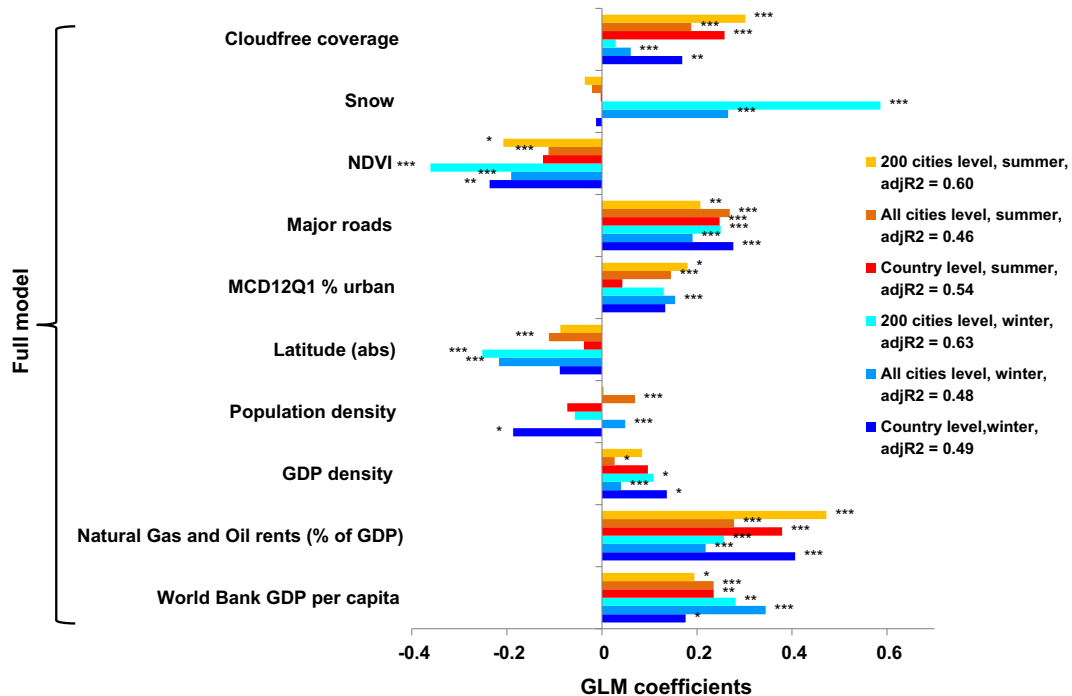

Fig. 10. Coefficients of socio-economic and physical variables included in full GLM analysis of cities' night-time brightness, for the winter and summer seasons, at the country level, for all cities, and for the 200 largest cities. (***p < 0.001, **p < 0.01, *p < 0.05).
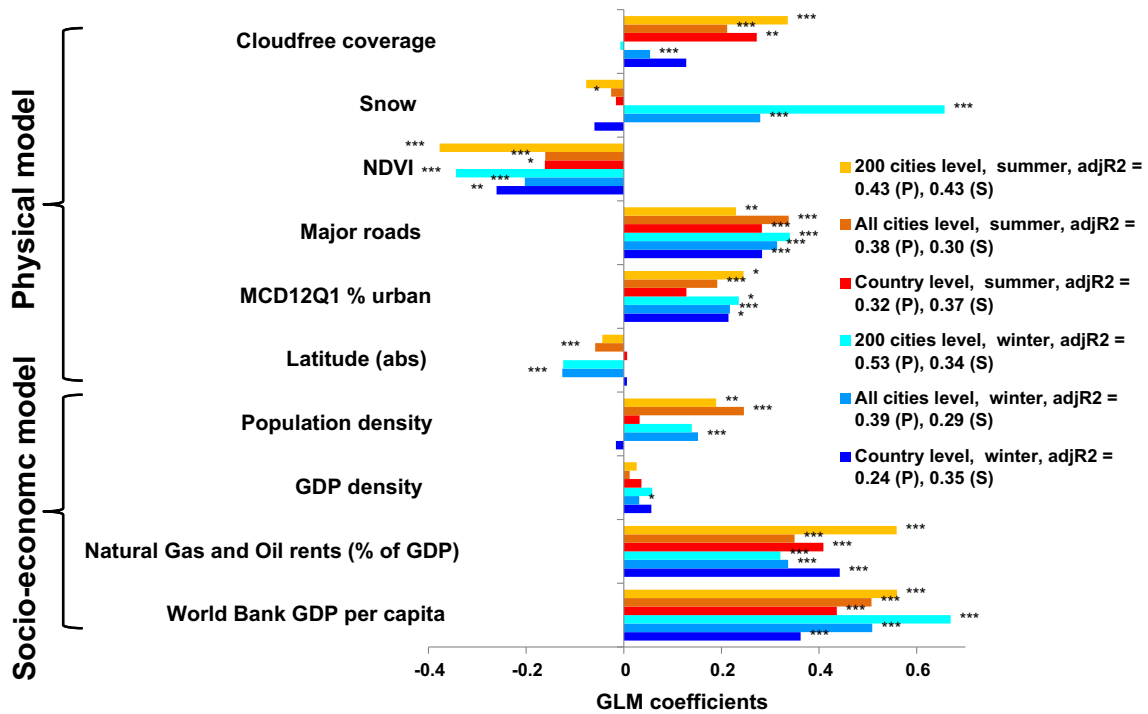
Fig. 11. Coefficients of socio-economic and physical variables included in separate GLM analysis of cities' night-time brightness, for the winter and summer seasons, at the country level, for all cities, and for the 200 largest cities. The parentheses after the adjusted R squared values in the legend represent whether they are for a model including only physical variables (P), or for a model including only socio-economic variables (S). (***p < 0.001, **p < 0.01, *p < 0.05).

positively correlated with nighttime brightness. Higher NDVI values in urban areas may indicate greater foliage cover, which can partly or fully block upward light emission (Bennie et al., 2014b), or large vegetated areas (e.g., grassy areas) whose low reflectance will decrease the reflectance of artificial lights towards the sky. This effect of vegetation cover on a city's night-time brightness as observed from space was recently reported using an EROS-B night-time image of Jerusalem (Katz and Levin, 2016). Cities in the countries surrounding the Persian Gulf often show low NDVI values (they are mainly located in an arid region), which might be one of the factors further enhancing the observed nighttime

brightness of these cities. In contrast with vegetation, snow cover leads to increased land surface reflectance in the visible and near-infrared ranges, increasing the upwards reflectance of downward lights (as demonstrated in Fig. 17) and thus enhancing the radiance measured by space-borne sensors (Román and Stokes, 2015). Indeed, snow cover has been reported to increase surface albedo by as much as 350% (Robinson and Kukla, 1985). While the increase in night-time brightness in January (with respect to July) of northern high latitude cities can be explained by snow cover in winter time (Fig. 6b; see Wu et al., 2013), some low latitude areas (especially India) presented some increase (in percentages
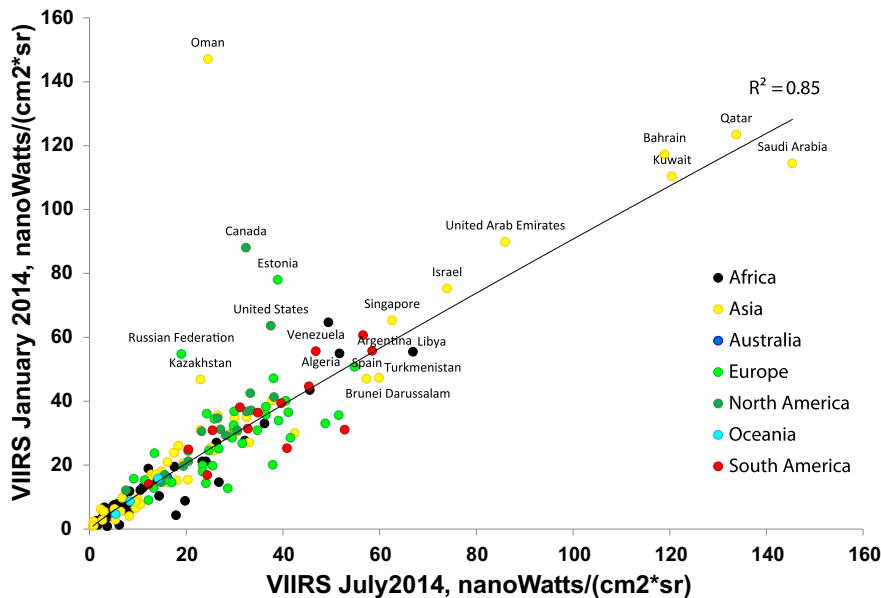

Fig. 12. Mean VIIRS radiance values in January 2014 at the country level (i.e. averaging all cities within a country), as a function of mean VIIRS radiance values in July 2014 (mean value for the urban areas of each country).
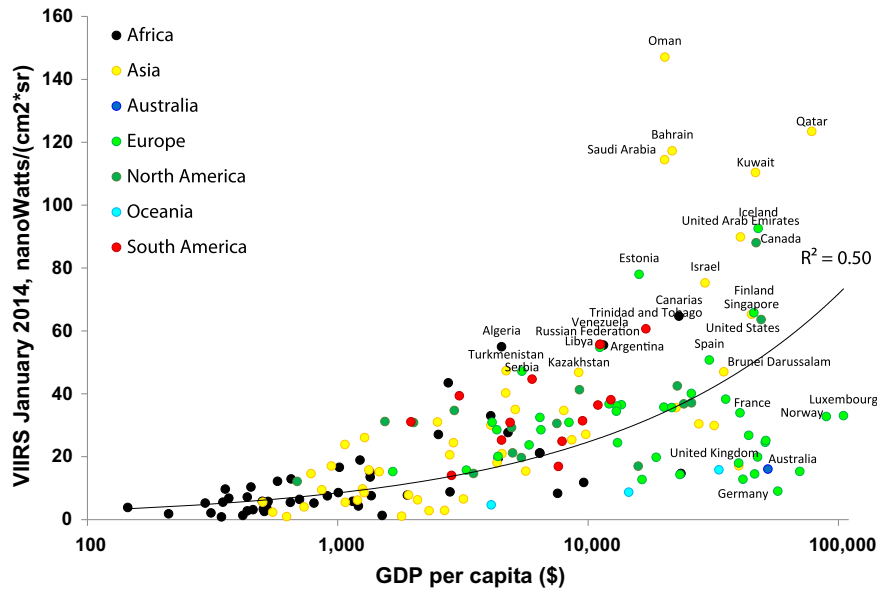
Fig. 13. Mean VIIRS radiance values in January 2014 at the country level (i.e. averaging all cities within a country), as a function of national GDP per capita.

more than in absolute values) in night-time brightness from July to January. This may be related to more consistent cloud coverage during the summer months (monsoon season) in India (Wilson and Jetz, 2016), hampering night-time observations of cities' brightness. This assumption is partly supported in our GLM analysis, where the number of cloud-free observations used to construct the monthly mosaics of the VIIRS, was positively correlated with cities' night-time brightness (Figs. 10, 11). Latitudinal differences in cities' night-time brightness may be explained not only by greater snow cover in high latitudes and persistent cloud cover in tropical latitudes, but also by seasonal changes in lighting strategy due to longer nights in high latitudes (Gaston et al., 2012; Wu et al., 2013).

Most studies on nighttime light brightness used lit area and not radiance calibrated values of brightness, because previous sources of remotely sensed images of nighttime lights (DMSP, astronaut photographs from the ISS, SAC-C images) were mostly not calibrated (but see Doll et al., 2006, where calibrated radiances from DMSP were used to map regional

economic activity from night-time imagery). The DNB band of the VIIRS onboard the Suomi NPP satellite presents a breakthrough in our ability to map the world at night (Miller et al., 2013), and is the first mission providing monthly average radiance composite images (available for downloading from http://ngdc.noaa.gov/eog/viirs/download_monthly.html, accessed on 22/7/2015). Cities' mean brightness levels were not linearly correlated with percent lit area, however both variables were found to be highly correlated with the explanatory variables examined here. Differences between using these two variables (percent lit area, mean brightness levels) were mostly noted when setting high threshold values; when thresholds of brightness levels were set high (above $100 \, nW/(cm^2 *sr)$), correlations between all explanatory variables and percent lit area decreased, except for the physical variables of snow cover and NDVI.

Our finding that multiple factors can affect nighttime light brightness at the city level confirms the findings of other studies at the country level (Wu et al., 2013; Ma et al., 2012). Given the fact that
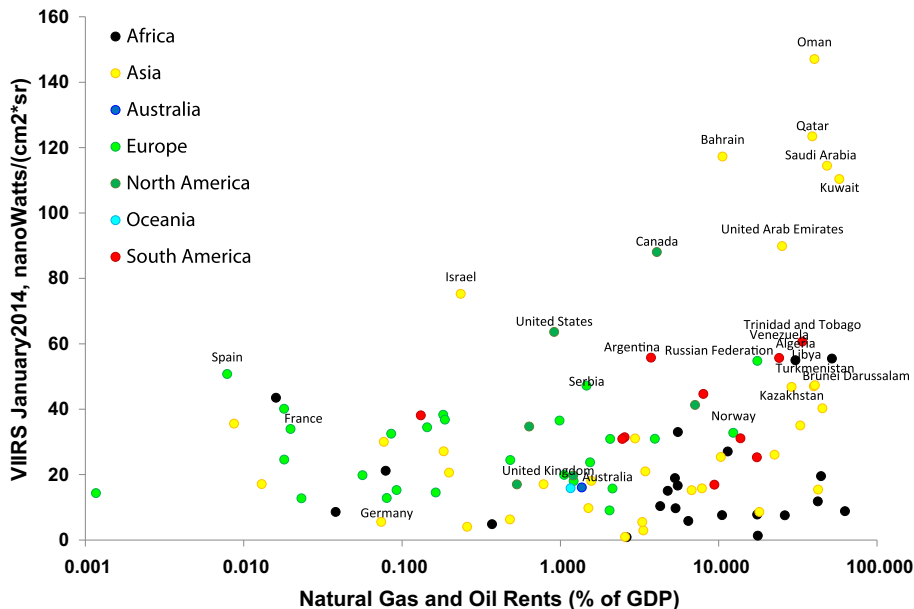

Fig. 14. Mean VIIRS radiance values in January 2014 at the country level (i.e. averaging all cities within a country), as a function of percent of GDP from natural gas and oil rents.
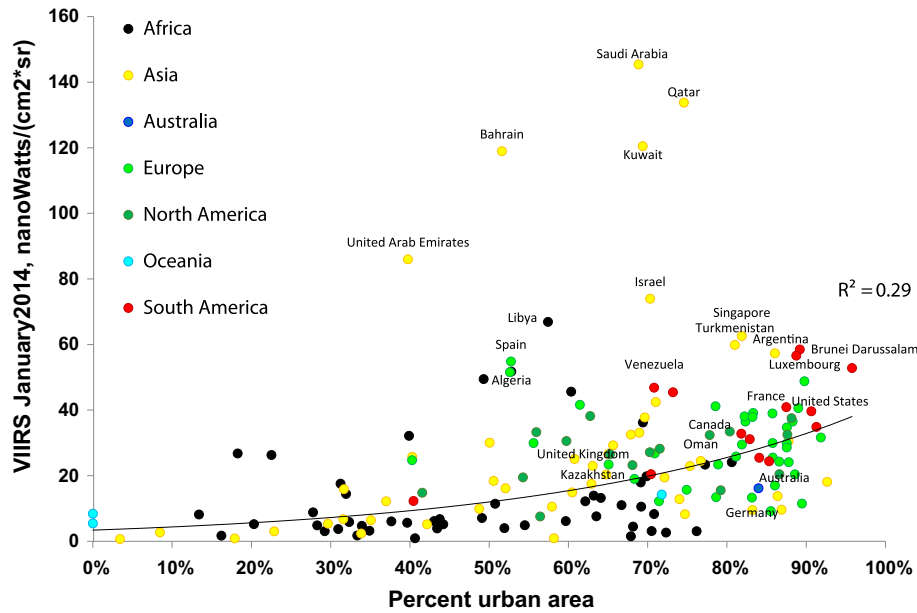
Fig. 15. Mean VIIRS radiance values in July 2014 at the country level (i.e. averaging all cities within a country), as a function of percent urban area (mean value for the cities of each country).

some studies have looked into predicting GDP with nighttime lights (Chen and Nordhaus, 2011; Elvidge et al., 1997; Shi et al., 2014a; Sutton et al., 2007), our findings suggest that caution must be taken when interpreting monthly nighttime lights as a proxy for economic activity, because there are additional factors which drive the emissions night lights besides economic activity. Indeed, Bickenbach et al. (2013) concluded that night lights data may be poor proxies for regional GDP. Due to the phenological cycle of vegetation and seasonal changes in snow cover, variations which are not related to the emission of nighttime lights can be introduced into nighttime light time series. Such variations must be first identified and decoupled from nighttime light time series before they can be used to track real seasonal changes in nighttime lights, which have been used to track human activities, such as holiday celebrations (Zhang et al., 2015; Román and Stokes, 2015) or seasonal

population gathering around cities in Africa (Bharti et al., 2011). Given the availability of a monthly cloud-free night-time lights product from VIIRS, we call for further studies to examine the effects of seasonal changes on nighttime lights intensity observed from space, using time series approaches which have been developed in recent years for analyzing vegetation (e.g., Verbesselt et al., 2010). Seasonal changes in observed night-light may be due to changes in surface reflectivity (e.g., snow and vegetation cover) or due to seasonal changes in human activity, and separating these factors is a challenge for the remote sensing community.

5. Conclusions

Nighttime light remote sensing is still in its infancy stage and is basically qualitative, compared with daytime optical remote sensing and
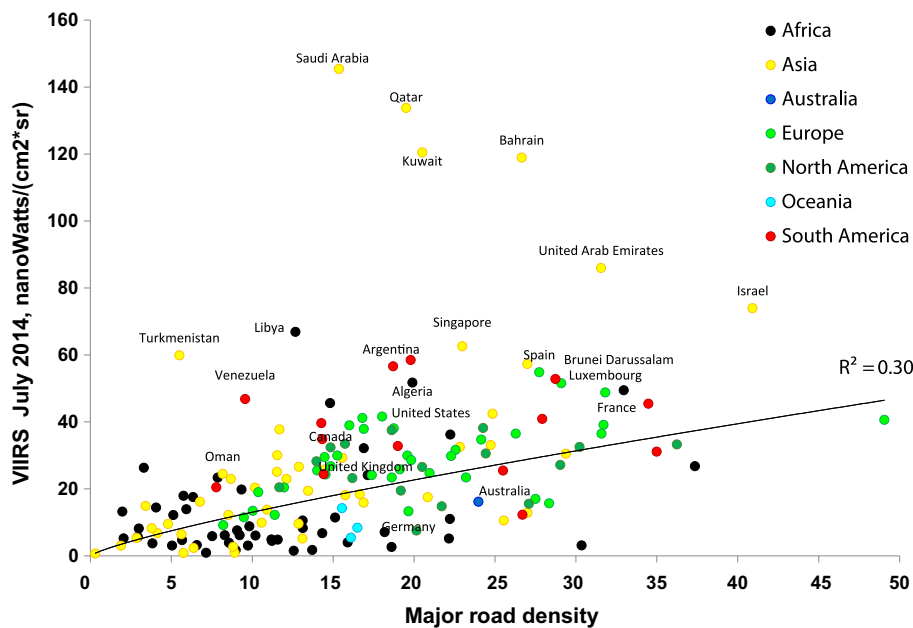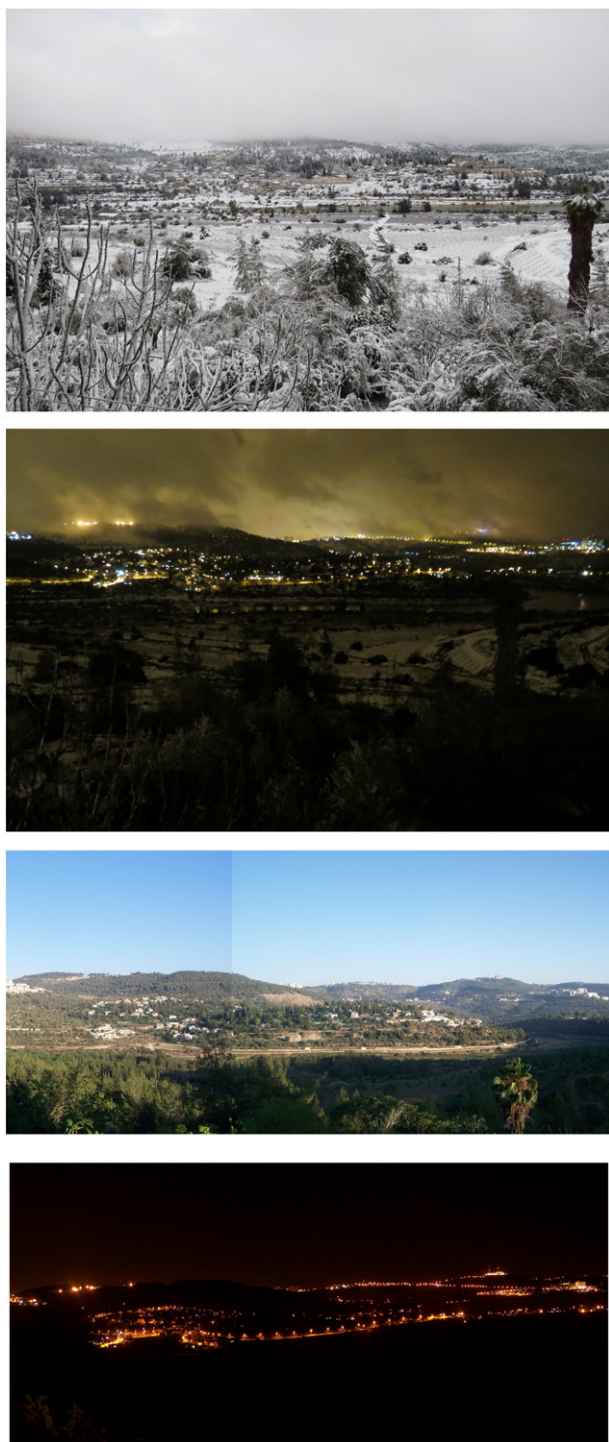

Fig. 16. Mean VIIRS radiance values in July 2014 at the country level (i.e. averaging all cities within a country), as a function of OpenStreetMap major road density (mean value for the urban areas of each country).

microwave remote sensing. There is still a lack of understanding of the mechanisms behind nighttime light remote sensing, due to the lack of studies at the ground level and the relative lack of understanding of nighttime light transfer from lighting sources through the air to the sensor. To advance nighttime light remote sensing, there is an urgent need for studies on factors that can influence nighttime light variation. With its dynamic radiometric range and advanced onboard calibration facilities, VIIRS takes continuous and consistent measurements of nighttime lights with significantly improved data quality, making the call for newer generation algorithms more urgent. Our current analysis is a direct response to that call.

We have shown that cities' night-light brightness is a function not only of fixed variables at both the country scale (e.g., GDP) and the city scale (e.g., density of the road network), but also of factors that have seasonal patterns, such as vegetation and snow cover. Our findings demonstrate some of the new insights which are now becoming possible thanks to the availability of global monthly radiance calibrated night-light mosaics from the VIIRS. Our findings suggest that in order to understand spatial and temporal variation in nighttime light intensity measured from space it is critical to first identify and separate variations caused by phenological cycles of vegetation and snow cover, as well as by moon lighting. This is especially important for applications to track human activities over time with nighttime light time series data. The next step is to quantitatively model factors that can influence nighttime light intensity in order to extract true light signals on the ground from nighttime light remote sensing imagery.

Acknowledgments

Appendix A. Supplementary data

Supplementary data associated with this article can be found in the online version, at http://dx.doi.org/10.1016/j.rse.2017.01.006. These data include the Google map of the densely populated areas ("cities") described in this article.

Fig. 17. Motsa Valley, on the western outskirts of Jerusalem, Israel. Snow covered at daytime (20/2/2015, 2:50 pm, exposure time of 1/125 s) and at night-time (21/2/2015, 2:57 am, exposure time of 1/4 s). The night-time photo demonstrates light-pollution under snow-cover conditions, due to increased surface reflectance. Notice that during the summer season (10/7/2008, 7:00 pm and 3:00 am), the valley is very dark at night-time, with no observed surface reflectance, due to low albedo of vegetation cover. Note that in addition to differences in snow cover, the winter photos show considerable downward atmospheric scattering of light from clouds which amplify light pollution (Kyba et al., 2011), while the summer photos show clear skies with negligible downward atmospheric scattering. All photos were taken by NL, using a Kodak Easyshare ZD710 (in 2008) and a Canon PowerShot SX40 HS (in 2015). It should be noted that snowfall is a rare event in Jerusalem, with two days of snow a year on average (Bitan and Ben-Rubi, 1978).

References

Angel, S., Parent, J., Civco, D.L., Blei, A., Potere, D., 2011. The dimensions of global urban expansion: Estimates and projections for all countries, 2000–2050. Prog. Plan. 75 (2), 53–107.
Baugh, K., Hsu, F.C., Elvidge, C.D., Zhizhin, M., 2013. Nighttime Lights Compositing Using the VIIRS Day-Night Band: Preliminary Results. Proceedings of the Asia-Pacific Advanced Network 35 pp. 70–86.
Bennie, J., Davies, T.W., Duffy, J.P., Inger, R., Gaston, K.J., 2014a. Contrasting trends in light pollution across Europe based on satellite observed night time lights. Sci. Rep. http://dx.doi.org/10.1038/srep03789.
Bennie, J., Davies, T.W., Inger, R., Gaston, K.J., 2014b. Mapping artificial lightscapes for ecological studies. Methods Ecol. Evol. 5 (6), 534–540.
Bhaduri, B., Bright, E., Coleman, P., Dobson, J., 2002. LandScan: Locating people is what matters. Geoinformatics 5, 34–37.
Bharti, N., Tatem, A.J., Ferrari, M.J., Grais, R.F., Djibo, A., Grenfell, B.T., 2011. Explaining seasonal fluctuations of measles in Niger using nighttime lights imagery. Science 334, 1424–1427.
Bickenbach, F., Bode, E., Lange, M., Nunnenkamp, P., 2013. Night Lights and Regional GDP (No. 1888). Kiel Working Paper.
Bitan, A., Ben-Rubi, P., 1978. The distribution of snow in Israel. GeoJournal 2 (6), 557–567.
Chan, K.W., Hu, Y., 2003. Urbanization in China in the 1990s: new definition, different series, and revised trends. China Rev. 3, 49–71.
Chen, X., Nordhaus, W.D., 2011. Using luminosity data as a proxy for economic statistics. Proc. Natl. Acad. Sci. 108 (21), 8589–8594.
Chen, Z., Yu, B., Hu, Y., Huang, C., Shi, K., Wu, J., 2015. Estimating house vacancy rate in metropolitan areas using NPP-VIIRS nighttime light composite data. IEEE J. Sel. Top. Appl. Earth Obs. Remote Sens. 8 (5), 2188–2197.

Cinzano, P., Falchi, F., Elvidge, C.D., 2001. The first world atlas of the artificial night sky brightness. Mon. Not. R. Astron. Soc. 328, 689–707.

Croft, T., 1978. Nighttime images of the earth from space. Sci. Am. 239, 86–98.

Didan, K., 2015. MOD13C2 MODIS/Terra Vegetation Indices Monthly L3 Global 0.05Deg CMG V006. NASA EOSDIS Land Processes DAAC. http://dx.doi.org/10.5067/MODIS/MOD13C2.006.

Doll, C.N., 2008. CIESIN Thematic Guide to Night-Time Light Remote Sensing and Its Applications. Center for International Earth Science Information Network of Columbia University, Palisades, NY.

Doll, C.N., Muller, J.P., Morley, J.G., 2006. Mapping regional economic activity from nighttime light satellite imagery. Ecol. Econ. 57 (1), 75–92.

Doukas, H., Patlitzianas, K.D., Kagiannas, A.G., Psarras, J., 2006. Renewable energy sources and rationale use of energy development in the countries of GCC: myth or reality? Renew. Energy 31 (6), 755–770.

Elvidge, C., Baugh, K., Kihn, E., Kroehl, H., Davis, E., Davis, C., 1997. Relation between satellite observed visible-near infrared emissions, population, economic activity and electric power consumption. Int. J. Remote Sens. 18, 1373–1379.

Elvidge, C.D., Baugh, K.E., Dietz, J.B., Bland, T., Sutton, P.C., Kroehl, H.W., 1999. Radiance calibration of DMSP-OLS low-light imaging data of human settlements. Remote Sens. Environ. 68 (1), 77–88.

Elvidge, C.D., Keith, D.M., Tuttle, B.T., Baugh, K.E., 2010. Spectral identification of lighting type and character. Sensors 10, 3961–3988.

Elvidge, C.D., Baugh, K.E., Zhizhin, M., Hsu, F.C., 2013. Why VIIRS Data Are Superior to DMSP for Mapping Nighttime Lights. Proceedings of the Asia-Pacific Advanced Network 35 pp. 62–69.

Elvidge, C.D., Zhizhin, M., Baugh, K., Hsu, F.C., Ghosh, T., 2016. Methods for global survey of natural gas flaring from visible infrared imaging radiometer suite data. Energies 9 (1):14. http://dx.doi.org/10.3390/en9010014.

Falchi, F., Cinzano, P., Elvidge, C.D., Keith, D.M., Haim, A., 2011. Limiting the impact of light pollution on human health, environment and stellar visibility. J. Environ. Manag. 92, 2714–2722.

Forstall, R.L., Greene, R.P., Pick, J.B., 2009. Which are the largest? Why lists of major urban areas vary so greatly. Tijdschr. Econ. Soc. Geogr. 100 (3), 277–297.

Gaffin, S.R., Rosenzweig, C., Xing, X., Yetman, G., 2004. Downscaling and geo-spatial gridding of socio-economic projections from the IPCC Special Report on Emissions Scenarios (SRES). Glob. Environ. Chang. 14 (2), 105–123.

Gaston, K.J., Davies, T.W., Bennie, J., Hopkins, J., 2012. Review: Reducing the ecological consequences of night-time light pollution: options and developments. J. Appl. Ecol. 49 (6), 1256–1266.

Gaston, K.J., Bennie, J., Davies, T.W., Hopkins, J., 2013. The ecological impacts of nighttime light pollution: a mechanistic appraisal. Biol. Rev. 88, 912–927.

Grimm, N.B., Faeth, S.H., Golubiewski, N.E., Redman, C.L., Wu, J., Bai, X., Briggs, J.M., 2008. Global change and the ecology of cities. Science 319 (5864), 756–760.

Haklay, M., 2010. How good is volunteered geographical information? A comparative study of OpenStreetMap and Ordnance Survey datasets. Environ. Plann. B. Plann. Des. 37 (4), 682–703.

Hale, J.D., Davies, G., Fairbrass, A.J., Matthews, T.J., Rogers, C.D., Sadler, J.P., 2013. Mapping lightscapes: spatial patterning of artificial lighting in an urban landscape. PloS ONE 8, e61460. http://dx.doi.org/10.1371/journal.pone.0061460.

Hernández-Henríquez, M.A., Déry, S.J., Derksen, C., 2015. Polar amplification and elevation-dependence in trends of Northern Hemisphere snow cover extent, 1971–2014. Environ. Res. Lett. 10 (4), 044010.

Huang, Q., Yang, X., Gao, B., Yang, Y., Zhao, Y., 2014. Application of DMSP/OLS nighttime light images: a meta-analysis and a systematic literature review. Remote Sens. 6 (8), 6844–6866.

Ibisch, P.L., Hoffmann, M.T., Kreft, S., Pe'er, G., Kati, V., Biber-Freudenberger, L., DellaSala, D.A., Vale, M.M., Hobson, P.R., Selva, N., 2016. A global map of roadless areas and their conservation status. Science 354:1423–1427. http://dx.doi.org/10.1126/science.aaf7166.

Jones, T.L., 2000. Compact city policies for megacities: core areas and metropolitan regions. In: Jenks, M., Burgess, R. (Eds.), Compact Cities: Sustainable Urban Forms for Developing Countries. SPON Press, London and New York, pp. 37–52.

Katz, Y., Levin, N., 2016. Quantifying urban light pollution - a comparison between field measurements and EROS-B imagery. Remote Sens. Environ. 177:65–77. http://dx.doi.org/10.1016/j.rse.2016.02.017.

Keola, S., Andersson, M., Hall, O., 2015. Monitoring economic development from space: Using nighttime light and land cover data to measure economic growth. World Dev. 66, 322–334.

Kim, M., 2012. Modeling nightscapes of designed spaces – case studies of the University of Arizona and Virginia Tech campuses. 13th International Conference on Information Technology in Landscape Architecture Proceedings, pp. 455–463.

Kuechly, H.U., Kyba, C., Ruhtz, T., Lindemann, C., Wolter, C., Fischer, J., Hölker, F., 2012. Aerial survey and spatial analysis of sources of light pollution in Berlin, Germany. Remote Sens. Environ. 126, 39–50.

Kyba, C.C., Ruhtz, T., Fischer, J., Hölker, F., 2011. Cloud coverage acts as an amplifier for ecological light pollution in urban ecosystems. PLoS One 6 (3), e17307.

Kyba, C., Garz, S., Kuechly, H., de Miguel, A.S., Zamorano, J., Fischer, J., Hölker, F., 2014. High-resolution imagery of Earth at night: new sources, opportunities and challenges. Remote Sens. 7 (1), 1–23.

Levin, N., Duke, Y., 2012. High spatial resolution night-time light images for demographic and socio-economic studies. Remote Sens. Environ. 119, 1–10.

Levin, N., Phinn, S., 2016. Illuminating the capabilities of Landsat 8 for mapping night lights. Remote Sens. Environ. 182, 27–38.

Levin, N., Kasper, J., Hacker, J.M., Phinn, S., 2014. A new source for high spatial resolution night time images - the EROS-B commercial satellite. Remote Sens. Environ. 149, 1–12.

Levin, N., Kark, S., Crandall, D., 2015. Where have all the people gone? Enhancing global conservation using night lights and social media. Ecol. Appl. 25 (8), 2153–2167.

Li, X., Xu, H., Chen, X., Li, C., 2013. Potential of NPP-VIIRS nighttime light imagery for modeling the regional economy of China. Remote Sens. 5, 3057–3081.

Lo, C.P., 2002. Urban indicators of China from radiance-calibrated digital DMSP-OLS nighttime images. Ann. Assoc. Am. Geogr. 92 (2), 225–240.

Longcore, T., Rich, C., 2004. Ecological light pollution. Front. Ecol. Environ. 2, 191–198.

Ma, T., Zhou, C., Pei, T., Haynie, S., Fan, J., 2012. Quantitative estimation of urbanization dynamics using time series of DMSP/OLS nighttime light data: A comparative case study from China's cities. Remote Sens. Environ. 124, 99–107.

Ma, T., Zhou, C., Pei, T., Haynie, S., Fan, J., 2014a. Responses of Suomi-NPP VIIRS-derived nighttime lights to socioeconomic activity in China's cities. Remote Sens. Lett. 5 (2), 165–174.

Ma, T., Zhou, Y., Wang, Y., Zhou, C., Haynie, S., Xu, T., 2014b. Diverse relationships between Suomi-NPP VIIRS night-time light and multi-scale socioeconomic activity. Remote Sens. Lett. 5 (7), 652–661.

Ma, T., Zhou, Y., Zhou, C., Haynie, S., Pei, T., Xu, T., 2015. Night-time light derived estimation of spatio-temporal characteristics of urbanization dynamics using DMSP/OLS satellite data. Remote Sens. Environ. 158, 453–464.

Mehrara, M., 2007. Energy consumption and economic growth: The case of oil exporting countries. Energy Policy 35 (5), 2939–2945.

de Miguel, A.S., 2015. Variación Espacial, Temporal y Espectral de la Contaminación Lumínica y Sus Fuentes: Metodología y Resultados. (PhD Thesis). Universidad Complutense de Madrid http://dx.doi.org/10.13140/RG.2.1.2233.7127.

de Miguel, A.S., Castaño, J.G., Zamorano, J., Pascual, S., Ángeles, M., Cayuela, L., ... Kyba, C.C., 2014. Atlas of astronaut photos of Earth at night. Astron. Geophys. 55 (4), 4–36.

Miller, S.D., Mills, S.P., Elvidge, C.D., Lindsey, D.T., Lee, T.F., Hawkins, J.D., 2012. Suomi satellite brings to light a unique frontier of nighttime environmental sensing capabilities. Proceedings of the National Academy of Sciences. 109, pp. 15706–15711.

Miller, S.D., Straka, W., Mills, S.P., Elvidge, C.D., Lee, T.F., Solbrig, J., ... Weiss, S.C., 2013. Illuminating the capabilities of the suomi national polar-orbiting partnership (NPP) visible infrared imaging radiometer suite (VIIRS) day/night band. Remote Sens. 5 (12), 6717–6766.

Neis, P., Zielstra, D., 2014. Recent developments and future trends in volunteered geographic information research: the case of OpenStreetMap. Future Internet 6 (1), 76–106.

Parilla, J., Trujillo, J.L., Berube, A., Ran, T., 2015. Global Mertomonitor 2014, an Uncertain Recovery. Metropolitan Policy Program. The Brookings Institution, Washington D.C.

Potere, D., Schneider, A., Angel, S., Civco, D.L., 2009. Mapping urban areas on a global scale: which of the eight maps now available is more accurate? Int. J. Remote Sens. 30 (24), 6531–6558.

Ramm, F., 2015. OpenStreetMap Data in Layered GIS Format Version 0.6.6 - 2015-07-06.

Reiche, D., 2010. Energy Policies of Gulf Cooperation Council (GCC) countries—possibilities and limitations of ecological modernization in rentier states. Energy Policy 38 (5), 2395–2403.

Robinson, D.A., Kukla, G., 1985. Maximum surface albedo of seasonally snow-covered lands in the Northern Hemisphere. J. Clim. Appl. Meteorol. 24 (5), 402–411.

Román, M.O., Stokes, E.C., 2015. Holidays in lights: Tracking cultural patterns in demand for energy services. Earth's Future 3 (6), 182–205.

Rouse, J.W., Haas, R.H., Schell, J.A., Deering, D.W., 1973. Monitoring Vegetation Systems in the Great Plains with ERTS', Third ERTS Symposium. NASA, pp. 309–317 (SP-351 I).

Shi, K., Yu, B., Huang, Y., Hu, Y., Yin, B., Chen, Z., Chen, L., Wu, J., 2014b. Evaluating the ability of NPP-VIIRS nighttime light data to estimate the gross domestic product and the electric power consumption of China at multiple scales: a comparison with DMSP-OLS data. Remote Sens. 6, 1705–1724.

Shi, K., Huang, C., Yu, B., Yin, B., Huang, Y., Wu, J., 2014a. Evaluation of NPP-VIIRS night-time light composite data for extracting built-up urban areas. Remote Sens. Lett. 5 (4), 358–366.

Small, C., Pozzi, F., Elvidge, C.D., 2005. Spatial analysis of global urban extent from DMSP-OLS night lights. Remote Sens. Environ. 96 (3), 277–291.

Southworth, M., Ben-Joseph, E., 1995. Street standards and the shaping of suburbia. J. Am. Plan. Assoc. 61 (1), 65–81.

Strahler, A., Muchoney, D., Borak, J., Friedl, M., Gopal, S., Lambin, E., Moody, A., 1999. MODIS Land Cover Product Algorithm Theoretical Basis Document (ATBD) Version 5.0 - MODIS Land Cover and Land-Cover Change.

Sutton, P.C., Elvidge, C.D., Ghosh, T., 2007. Estimation of gross domestic product at sub-national scales using nighttime satellite imagery. International Journal of Ecological Economics & Statistics 8 (S07), 5–21.

Verbesselt, J., Hyndman, R., Newnham, G., Culvenor, D., 2010. Detecting trend and seasonal changes in satellite image time series. Remote Sens. Environ. 114 (1), 106–115.

Weidmann, N.B., Schutte, S., 2016. Using night light emissions for the prediction of local wealth. J. Peace Res. (0022343316630359), http://dx.doi.org/10.1177/0022343316630359.

Wilson, A.M., Jetz, W., 2016. Remotely sensed high-resolution global cloud dynamics for predicting ecosystem and biodiversity distributions. PLoS Biol. 14 (3), e1002415.

Wu, J., Wang, Z., Li, W., Peng, J., 2013. Exploring factors affecting the relationship between light consumption and GDP based on DMSP/OLS nighttime satellite imagery. Remote Sens. Environ. 134, 111–119.

Zhang, Q., Seto, K.C., 2013. Can night-time light data identify typologies of urbanization? A global assessment of successes and failures. Remote Sens. 5 (7), 3476–3494.

Zhang, Q., Levin, N., Chalkias, C., Letu, H., 2015. Nighttime light remote sensing – monitoring human societies from outer space. (Chapter 11). In: Thenkabail, P.S. (Ed.), Remote Sensing Handbook vol. 3. Taylor and Francis, pp. 289–310.